Proceedings of IDETC/CIE 2005
ASME 2005 International Design Engineering Technical Conferences
& Computers and Information in Engineering Conference
September 24-28, 2005, Long Beach, California USA

DETC2005-84524

CROSS-SECTION DEFORMATION IN THE ABSOLUTE NODAL COORDINATE FORMULATION

Hiroyuki Sugiyama
Department of Mechanical Engineering
University of Illinois at Chicago
842 West Taylor Street
Chicago, Illinois 60667

Johannes Gerstmayr
Institute for Technical Mechanics
Johannes Kepler University of Linz
Altenbergerstr. 69
4040 Linz, Austria

Ahmed A. Shabana
Department of Mechanical Engineering
University of Illinois at Chicago
842 West Taylor Street
Chicago, Illinois 60667

ABSTRACT

In this investigation, the deformation modes defined in the finite element absolute nodal coordinate formulation using several strain definitions are discussed. In order to accurately define strain components that can have easy physical interpretation, a material coordinate system is introduced to define the material element rotation and deformation. The results obtained in this study clearly show cross-section deformation modes eliminated when the number of the finite element nodal coordinates is systematically and consistently reduced. Using the procedure discussed in this paper, one can obtain a reduced order dynamic model, eliminate position vector gradients that introduce high frequencies to the solution of some problems, achieve the continuity of the remaining gradients at the nodal points, and obtain a formulation that automatically satisfies the principle of work and energy.

1 INTRODUCTION

In the absolute nodal coordinate formulation, only the position field is interpolated in order to define a unique rotation field that can be determined using the position vector gradients [1]. Therefore, finite rotation parameters are not interpolated and are not used as nodal coordinates. The gradients, as the result of the *Polar Decomposition Theorem* [2], can be used to define a unique rotation field within the element as well as at the element boundaries and nodes. By so doing, the problem of coordinate redundancy that characterizes existing large deformation finite element formulations that interpolate finite rotation parameters can be avoided. For this reason, the solution obtained using the absolute nodal coordinate formulation does not lead to energy drift or violation of the principle of work and energy as it is the case in many existing methods.

While the absolute nodal coordinate formulation can be and has been successfully used in many large deformation and large rotation applications, numerical problems can be encountered in some applications that include very thin and very stiff structures. These numerical problems are the result of high frequency oscillations induced by the change in gradients used to describe some of the element cross-section deformation modes. While implicit time integrations [3,4], reduced order integrations and the lower order elements [5-7] can be used to solve these numerical problems, another approach that can be followed and is adopted in this investigation is to use the strain definitions to obtain conditions that can be used to eliminate the insignificant deformation modes of the element cross-section. To this end, local strain components defined in local frames are first defined and used to shed light on the cross-section deformation modes. Using these strain definitions, different models with different orders can be defined by imposing algebraic conditions that can be used to eliminate some of the element cross-section deformation degrees of freedom. It is shown that some of the existing models such as Reissner and Euler-Bernoulli beam models can be systematically obtained from the general description used in the absolute nodal coordinate formulation. Furthermore, the reduction procedure described in this paper ensures the continuity of all the gradients at the nodal points. The reduction procedure, however, has several drawbacks that include a non-constant mass matrix, non-zero centrifugal and Coriolis forces and/or the need to solve a system of differential and algebraic equations. Therefore, the method discussed in this paper differs from the methods that employ the absolute nodal coordinate formulation with a smaller number of nodal coordinates and presented in previous investigations [5-7].

2 ABSOLUTE NODAL COORDINATE FORMULATION

In this investigation, a three-dimensional beam element is used in order to discuss the cross-section deformation modes in the absolute nodal coordinate formulation. The displacement field of a three-dimensional beam element can be interpolated using a polynomial cubic in x and polynomials linear in y and z as follows:

$$\mathbf{r} = \mathbf{r}^c + y\mathbf{w}^1 + z\mathbf{w}^2 \tag{1}$$

where $\mathbf{r}^c = \mathbf{S}_{\mathrm{I}}(x)\mathbf{e}$, $\mathbf{w}^1 = \mathbf{S}_{\mathrm{II}}(x)\mathbf{e}$, $\mathbf{w}^2 = \mathbf{S}_{\mathrm{III}}(x)\mathbf{e}$ and the shape function matrices used in this displacement field are,

respectively, defined as follows:

$$\mathbf{S}_{\mathrm{I}}(x)=\begin{bmatrix} s_1\mathbf{I} & s_2\mathbf{I} & \mathbf{0} & \mathbf{0} & s_3\mathbf{I} & s_4\mathbf{I} & \mathbf{0} & \mathbf{0}\end{bmatrix}$$
$$\mathbf{S}_{\mathrm{II}}(x)=\begin{bmatrix} \mathbf{0} & \mathbf{0} & \overline{s}_1\mathbf{I} & \mathbf{0} & \mathbf{0} & \mathbf{0} & \overline{s}_2\mathbf{I} & \mathbf{0}\end{bmatrix} \quad (2)$$
$$\mathbf{S}_{\mathrm{III}}(x)=\begin{bmatrix} \mathbf{0} & \mathbf{0} & \mathbf{0} & \overline{s}_1\mathbf{I} & \mathbf{0} & \mathbf{0} & \mathbf{0} & \overline{s}_2\mathbf{I}\end{bmatrix}$$

where

$$s_1=1-3\xi^2+2\xi^3, \quad s_2=\ell(\xi-2\xi^2+\xi^3)$$
$$s_3=3\xi^2-2\xi^3, \quad s_4=\ell(-\xi^2+\xi^3) \quad (3)$$
$$\overline{s}_1=1-\xi, \quad \overline{s}_2=\xi$$

and $\xi=x/\ell$ where ℓ is the length of the beam element in the undeformed configuration. It can be seen from the preceding equations that the shape functions are defined by cubic Hermite polynomials for the displacements along the beam centerline, while linear polynomials are used for the displacements of the beam cross-section.

Using the displacement field defined by Eq. 1, the matrix of the position vector gradients for the beam can be expressed as follows:

$$\mathbf{J}=\partial\mathbf{r}/\partial\mathbf{x} \quad (4)$$

where $\mathbf{x}=\begin{bmatrix} x & y & z\end{bmatrix}^T$. In the preceding equation, the gradients are obtained using differentiation with respect to the element coordinates *x*, *y*, and *z*. The matrix of gradients in Eq. 4 is related to the matrix of gradients $\mathbf{J}^g$ defined by differentiation with respect to $\mathbf{X}=\mathbf{S}\mathbf{e}_o$ given by $\mathbf{J}^g=\mathbf{J}\dfrac{\partial\mathbf{x}}{\partial\mathbf{X}}$, where $\mathbf{e}_o$ is the vector of nodal coordinates in the undeformed configuration. Assuming that the beam is initially straight and substituting Eq. 1 into Eq. 4, one has

$$\mathbf{J}=\begin{bmatrix}\mathbf{r}_x^c+y\mathbf{w}_x^1+z\mathbf{w}_x^2 & \mathbf{w}^1 & \mathbf{w}^2\end{bmatrix} \quad (5)$$

In this equation, subscript *x* indicates differentiation with respect to the element coordinate *x*; for example, $\mathbf{r}_x^c=\partial\mathbf{r}^c/\partial x$. It is clear from Eq. 5 that $\mathbf{w}^1$ and $\mathbf{w}^2$ define the position vector gradients associated with the spatial coordinates *y* and *z*. Therefore, the matrix of the position vector gradients of Eq. 5 can be written as

$$\mathbf{J}=\begin{bmatrix}\mathbf{r}_x^c+y\mathbf{r}_{yx}+z\mathbf{r}_{zx} & \mathbf{r}_y & \mathbf{r}_z\end{bmatrix} \quad (6)$$

where $\mathbf{r}_y=\partial\mathbf{r}/\partial y$ and $\mathbf{r}_z=\partial\mathbf{r}/\partial z$. It is important to note that, when using a shape function that is linear in *y* and *z*, the position vector gradient associated with the element coordinates *y* and *z* are defined by the following linear interpolations (see Eqs. 1-3):

$$\mathbf{r}_y=(1-\xi)\mathbf{r}_y^1+\xi\mathbf{r}_y^2, \quad \mathbf{r}_z=(1-\xi)\mathbf{r}_z^1+\xi\mathbf{r}_z^2 \quad (7)$$

where $\mathbf{r}_y^k$ and $\mathbf{r}_z^k$ (*k*=1,2) represent the gradient nodal coordinates at node *k*. On the other hand, the gradients associated with the spatial coordinate *x* are defined by $\mathbf{r}_x^c+y\mathbf{r}_{yx}+z\mathbf{r}_{zx}$. Since the position vector gradients associated with *y* and *z* are used to describe the large rigid body motion of the cross-section as well as the deformation, the use of the *y* and *z* linear interpolation leads to less accurate definition of strain components as will be discussed in later sections of this paper.

3 LAGRANGIAN STRAINS

Using the displacement gradients given by Eq. 6, the Green-Lagrange strain components can be obtained for an initially straight beam as [8]

$$\varepsilon^{11}=\frac{1}{2}\left(\mathbf{r}_x^c\cdot\mathbf{r}_x^c-1\right)+y\mathbf{r}_x^c\cdot\mathbf{r}_{yx}+z\mathbf{r}_x^c\cdot\mathbf{r}_{zx}+\varepsilon^{qx}$$
$$\varepsilon^{22}=\frac{1}{2}\left(\mathbf{r}_y\cdot\mathbf{r}_y-1\right), \quad \varepsilon^{33}=\frac{1}{2}\left(\mathbf{r}_z\cdot\mathbf{r}_z-1\right), \quad (8)$$
$$\varepsilon^{12}=\frac{1}{2}\left(\mathbf{r}_x^c\cdot\mathbf{r}_y+z\mathbf{r}_{zx}\cdot\mathbf{r}_y+y\mathbf{r}_{yx}\cdot\mathbf{r}_y\right)$$
$$\varepsilon^{13}=\frac{1}{2}\left(\mathbf{r}_x^c\cdot\mathbf{r}_z+z\mathbf{r}_{zx}\cdot\mathbf{r}_z+y\mathbf{r}_{yx}\cdot\mathbf{r}_z\right), \quad \varepsilon^{23}=\frac{1}{2}\mathbf{r}_y\cdot\mathbf{r}_z$$

where ε^{qx} is higher order shear strain components associated with the deformation of the cross-section. Note that the strain associated with pure elongation of a beam is defined by the one-dimensional Green strain:

$$\varepsilon^{nx}=\frac{1}{2}\left(\mathbf{r}_x^c\cdot\mathbf{r}_x^c-1\right) \quad (9)$$

where superscript *n* is used for the normal strain. Similarly, the normal strains produced by pure stretches of the cross-section planes along the *y* and *z* directions can be, respectively, expressed as

$$\varepsilon^{ny}=\frac{1}{2}\left(\mathbf{r}_y\cdot\mathbf{r}_y-1\right), \quad \varepsilon^{nz}=\frac{1}{2}\left(\mathbf{r}_z\cdot\mathbf{r}_z-1\right) \quad (10)$$

Shear strains due to the deformation of the beam cross-section are given by

$$\varepsilon^{sxy}=\frac{1}{2}\mathbf{r}_x^c\cdot\mathbf{r}_y, \quad \varepsilon^{sxz}=\frac{1}{2}\mathbf{r}_x^c\cdot\mathbf{r}_z \quad (11)$$

where superscript *s* refers to shear strains. Similarly, the shear strain in *y* and *z* plane is defined by

$$\varepsilon^{syz}=\frac{1}{2}\mathbf{r}_y\cdot\mathbf{r}_z \quad (12)$$

The remaining strain components are functions of deformation modes associated with bending, torsion, and twist of the cross-section. However, since the displacement gradients defined by Eq. 6 allow for the deformation of the cross-section, these strain definitions contain terms that include couplings between the rotation strain components and the deformation of the cross-section as can be seen from Eq. 8. For this reason, more detailed discussions on the deformation modes associated with the rotation strains will be provided in the following sections after introducing local material frames that can be used to conveniently provide a clear physical interpretation of the modes of deformation of the cross-section.

4 LOCAL MATERIAL FRAMES

In this section, a local finite element cross-section coordinate system is introduced in order to define local strain components. These strain components can be simplified in order to obtain the strain definitions used in Reissner's and Euler-Bernoulli beam theories used in many geometrically

exact beam element models [9-11]. The Polar Decomposition Theorem states that the matrix of position vector gradients can be written as the product of two matrices; an orthogonal matrix that defines the rigid body rotation and a stretch matrix that defines the strains and deformation. The orthogonal matrix that can be expressed in terms of three independent parameters defines a frame in which the gradients and strains can be defined. In this section, we consider two alternate forms that can be easily determined using the position vector gradients. These are the tangent frame and the cross-section frame.

Cross-Section and Tangent Frames A reference frame that can be used for the local definitions of the strains is the cross-section frame. It can be shown that an arbitrary vector defined on the cross-section can be expressed as a linear combination of the two vectors $\mathbf{r}_y$ and $\mathbf{r}_z$. Therefore, using Gram-Schmidt orthogonalization process and the position vector gradients, $\mathbf{r}_y$ and $\mathbf{r}_z$, one can define an orthonormal triad on the deformable beam cross-section as follows [1]:

$$\mathbf{j}^o = \frac{\mathbf{r}_y}{\left|\mathbf{r}_y\right|}, \quad \mathbf{k}^o = \frac{\mathbf{r}_z - h\mathbf{r}_y}{\left|\mathbf{r}_z - h\,\mathbf{r}_y\right|}, \quad \mathbf{i}^o = \mathbf{j}^o \times \mathbf{k}^o \tag{13}$$

where $h = \mathbf{r}_z{}^T\mathbf{r}_y / \mathbf{r}_y{}^T\mathbf{r}_y$. Accordingly, the orthonormal orientation matrix can be defined as follows:

$$\mathbf{A}^o = \begin{bmatrix} \mathbf{i}^o & \mathbf{j}^o & \mathbf{k}^o \end{bmatrix} \tag{14}$$

Another reference frame can be defined using the position vector gradients such that the first axis of the reference frame is always tangent to the beam centerline, $\mathbf{r}_x^c$. Such a coordinate system is called the tangent frame and is defined as follows [12]:

$$\mathbf{A}^t = \begin{bmatrix} \mathbf{i}^t & \mathbf{j}^t & \mathbf{k}^t \end{bmatrix} \tag{15}$$

where

$$\mathbf{i}^t = \frac{\mathbf{r}_x^c}{\left|\mathbf{r}_x^c\right|}, \quad \mathbf{k}^t = \frac{\hat{\mathbf{r}}_x^c \times \hat{\mathbf{r}}_y}{\left|\hat{\mathbf{r}}_x^c \times \hat{\mathbf{r}}_y\right|}, \quad \mathbf{j}^t = \mathbf{k}^t \times \mathbf{i}^t \tag{16}$$

where $\hat{\mathbf{a}}$ denotes a unit vector in the direction of the vector **a**, that is $\hat{\mathbf{a}} = \mathbf{a}/\left|\mathbf{a}\right|$. In the following, the cross-section and tangent frames will be referred to as the *local material frame* as shown in Fig. 1

QR Decomposition and the Stain Components In what follows, it is shown that the use of the tangent frame leads to the definition of the orthogonal matrix that appears in the **QR** decomposition of the matrix of the position vector gradients. That is, the matrix $\mathbf{A}^t$ is the orthogonal matrix **Q** that appears in the **QR** decomposition of the matrix of the position vector gradients **J** defined on the beam centerline, and **R** is an upper-triangular matrix. Using the tangent frame defined by Eqs. 15 and 16, the matrix of the position vector gradients **J** can be expressed as follows:

$$\mathbf{J} = \mathbf{A}^t\mathbf{U}^t \tag{17}$$

where $\mathbf{U}^t = (\mathbf{A}^t)^T\mathbf{J}$. Using the displacement gradients defined by Eq. 6 for the beam element, one can write

$$\mathbf{J} = \mathbf{J}^c + \mathbf{J}^p \tag{18}$$

where $\mathbf{J}^c$ is the matrix of the position vector gradients defined on the beam centerline, while $\mathbf{J}^p = \mathbf{J} - \mathbf{J}^c$ is a function of the *x*, *y* and *z* coordinates. The matrices $\mathbf{J}^c$ and $\mathbf{J}^p$ can be defined using the displacement field of Eq. 6 as

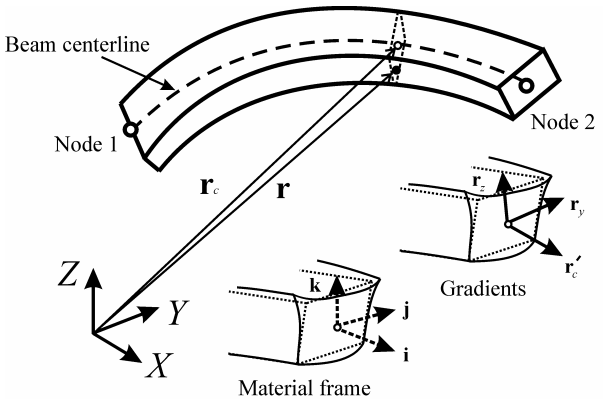

Fig. 1 Absolute nodal coordinates of the beam element

$$\mathbf{J}^c = \begin{bmatrix} \mathbf{r}_x^c & \mathbf{r}_y & \mathbf{r}_z \end{bmatrix}, \quad \mathbf{J}^p = \begin{bmatrix} \mathbf{r}_x^p & \mathbf{0} & \mathbf{0} \end{bmatrix} \tag{19}$$

where $\mathbf{r}_x^p(x, y, z) = y\mathbf{r}_{yx} + z\mathbf{r}_{zx}$. Using the decomposition given by Eq. 17, the matrix $\mathbf{U}^t$ can be obtained as

$$\mathbf{U}^t = (\mathbf{A}^t)^T\mathbf{J} = \mathbf{U}^{tc} + \mathbf{U}^{tp} \tag{20}$$

where

$$\begin{aligned} \mathbf{U}^{tc}(x) &= (\mathbf{A}^t)^T\mathbf{J}^c = \begin{bmatrix} \mathbf{i}^t\cdot\mathbf{r}_x^c & \mathbf{i}^t\cdot\mathbf{r}_y & \mathbf{i}^t\cdot\mathbf{r}_z \\ 0 & \mathbf{j}^t\cdot\mathbf{r}_y & \mathbf{j}^t\cdot\mathbf{r}_z \\ 0 & 0 & \mathbf{k}^t\cdot\mathbf{r}_z \end{bmatrix} \\ \mathbf{U}^{tp}(x, y, z) &= (\mathbf{A}^t)^T\mathbf{J}^p = \begin{bmatrix} \mathbf{i}^t\cdot\mathbf{r}_x^p & 0 & 0 \\ \mathbf{j}^t\cdot\mathbf{r}_x^p & 0 & 0 \\ \mathbf{k}^t\cdot\mathbf{r}_x^p & 0 & 0 \end{bmatrix} \end{aligned} \tag{21}$$

It is clear from Eq. 21 that, on the centerline of the beam, one has the following decomposition for the matrix of the position vector gradients that can be obtained using **QR** decomposition:

$$\mathbf{J}^c = \mathbf{A}^t\mathbf{U}^{tc} = \mathbf{QR} \tag{22}$$

where $\mathbf{U}^{tc}$ is an upper triangular matrix that depends on the strains. When first-order approximations are employed, one can have the following strain components projected on the tangent frame:

$$\boldsymbol{\varepsilon} \simeq \frac{1}{2}((\mathbf{U}^t)^T + \mathbf{U}^t) - \mathbf{I} \;\; \boldsymbol{\varepsilon} \simeq \frac{1}{2}((\mathbf{U}^t)^T + \mathbf{U}^t) - \mathbf{I} \tag{23}$$

It is clear from these linearized expressions that the contribution of the rotations of the cross-section to the longitudinal strain component is given by $\mathbf{i}^t\cdot\mathbf{r}_x^p = y\mathbf{i}^t\cdot\mathbf{r}_{yx} + z\mathbf{i}^t\cdot\mathbf{r}_{zx}$. However, since $\mathbf{r}_y$ and $\mathbf{r}_z$ are defined using a linear polynomial as given by Eq. 7 in the case of the beam element, the derivatives of $\mathbf{r}_y$ and $\mathbf{r}_z$ become constant along the length [13]. This linear interpolation leads to a less accurate definition of the bending strains when strain definitions given

by either Eqs. 8 or 23 are used. For this reason, as will be discussed in the following sections, the use of the curvature definitions given by $\overline{\kappa}_2 = -\mathbf{k}^T \dfrac{d\,\mathbf{i}}{ds}$, $\overline{\kappa}_3 = \mathbf{j}^T \dfrac{d\,\mathbf{i}}{ds}$ leads to more accurate definition of the bending strains since **i** is defined by the vector $\mathbf{r}_x^c$ which is approximated using cubic polynomials as shown in Eqs. 1-3, where *s* is the arc-length coordinate.

5 LOCAL STRAIN DEFINITIONS

In this section, the nonlinear strain components of the element cross-section are expressed using the local material frames in order to identify the rotation strain components and their coupling with the deformation of the cross-section. To this end, the gradients at the material point are projected on the material frames and simplifying assumptions regarding the deformation of the cross-section are made in order to provide the interpretation of the nonlinear strain components obtained using the absolute nodal coordinate formulation.

Curvature and Torsion The orientation of the Serret-Frenet frame associated with the spatial curve representing the beam centerline can be defined using the unit tangent **t**, normal **n**, and binormal **b**. The orientation of this frame can then be defined by the transformation matrix [14]

$$\mathbf{A}^f = \begin{bmatrix} \mathbf{t} & \mathbf{n} & \mathbf{b} \end{bmatrix} \tag{24}$$

From the theory of curves in differential geometry, one has the following expressions for the derivatives of **t**, **n** and **b** [14]

$$\mathbf{t}_s = \overline{\kappa}\mathbf{n}, \quad \mathbf{n}_s = -\overline{\kappa}\mathbf{t} + \overline{\tau}\mathbf{b}, \quad \mathbf{b}_s = -\overline{\tau}\mathbf{n} \tag{25}$$

where subscript *s* refers to differentiation with respect to the arc-length *s*, $\overline{\kappa}$ is the curvature and $\overline{\tau}$ is the torsion. Using the preceding two equations, one can show that

$$\tilde{\overline{\boldsymbol{\kappa}}} = (\mathbf{A}^f)^T \mathbf{A}_s^f \tag{26}$$

where $\tilde{\overline{\boldsymbol{\kappa}}}$ is the skew-symmetric matrix

$$\tilde{\overline{\boldsymbol{\kappa}}} = \begin{bmatrix} 0 & -\overline{\kappa} & 0 \\ \overline{\kappa} & 0 & -\overline{\tau} \\ 0 & \overline{\tau} & 0 \end{bmatrix} \tag{27}$$

It can be seen from the preceding equation that torsion is defined as rotation about the tangent **t**, while curvature is defined as rotation about the binormal **b**.

In the case of the tangent frame, one can write the transformation matrix $\mathbf{A}^t$ that defines the orientation of the tangent frame in the global coordinate system in terms of the matrix $\mathbf{A}^f$ that defines the orientation of the Serret-Frenet frame as follows:

$$\mathbf{A}^t = \mathbf{A}^f \mathbf{A}^{tf} \tag{28}$$

where $\mathbf{A}^{tf}$ is the matrix that defines the orientation of the tangent frame with respect to the Serret-Frenet frame. This matrix can be expressed in terms of one angle β as follows:

$$\mathbf{A}^{tf} = \begin{bmatrix} 1 & 0 & 0 \\ 0 & \cos\beta & -\sin\beta \\ 0 & \sin\beta & \cos\beta \end{bmatrix} \tag{29}$$

It follows that

$$\tilde{\overline{\boldsymbol{\kappa}}}^t = (\mathbf{A}^t)^T \mathbf{A}_s^t = \tilde{\overline{\boldsymbol{\kappa}}}^t = \begin{bmatrix} 0 & -\overline{\kappa}\cos\beta & \overline{\kappa}\cos\gamma \\ \overline{\kappa}\cos\beta & 0 & -\overline{\tau} \\ -\overline{\kappa}\cos\gamma & \overline{\tau} & 0 \end{bmatrix} \tag{30}$$

where $\tilde{\overline{\boldsymbol{\kappa}}}^t$ is the *curvature-torsion matrix* associated with the tangent frame and γ is an angle between the binormal **b** and the second axis of the tangent frame $\mathbf{j}^t$ given by $\gamma = \beta - \pi/2$. It is shown in Eq. 30 that when the tangent frame is used, the rotational component associated with the longitudinal axis remains the same as the torsion defined in Serret-Frenet frame, while the curvature defined about the binormal **b** is projected into two axes $\mathbf{j}^t$ and $\mathbf{k}^t$ that differ from the normal and binormal used in the Serret-Frenet frame.

In general, for any local material frame, by the virtue of the orthogonality of the transformation matrix $\mathbf{A} = \begin{bmatrix} \mathbf{i} & \mathbf{j} & \mathbf{k} \end{bmatrix}$ that defines the orientation of this frame ($\mathbf{A}^T\mathbf{A}=\mathbf{I}$), one always has

$$\tilde{\overline{\boldsymbol{\kappa}}} = \mathbf{A}^T \mathbf{A}_s \tag{31}$$

where $\tilde{\overline{\boldsymbol{\kappa}}}$ is a skew-symmetric matrix associated with the vector $\overline{\boldsymbol{\kappa}} = [\overline{\kappa}_1 \quad \overline{\kappa}_2 \quad \overline{\kappa}_3]^T$, where

$$\overline{\kappa}_1 = \mathbf{k}\cdot\mathbf{j}_s, \qquad \overline{\kappa}_2 = -\mathbf{k}\cdot\mathbf{i}_s, \qquad \overline{\kappa}_3 = \mathbf{j}\cdot\mathbf{i}_s \tag{32}$$

In these equations, subscript *s* indicates differentiation with respect to the arc-length parameter *s*. Note that the definition of the torsion and curvatures associated with the tangent and cross-section frames are different. Using the assumption that the longitudinal axis of the cross-section frame does not significantly differ from the tangent to the beam centerline, $\overline{\kappa}_1$ in the preceding equation can be assumed to represent the torsion. One, however, must ensure that the definition of torsion is correctly interpreted when the cross-section frame is used, particularly in the case of large deformation problems.

Local Strain Definitions The position vector gradients along *y* and *z* directions of the cross-section are projected on a local coordinate system attached to the material points as follows:

$$\overline{\mathbf{r}}^y = \mathbf{A}^T \mathbf{r}_y, \qquad \overline{\mathbf{r}}^z = \mathbf{A}^T \mathbf{r}_z \tag{33}$$

where the matrix **A** can be the transformation matrix that defines the cross-section or the tangent frame. Using the preceding equation, the matrix of position vector gradients of Eq. 6 can be written as

$$\mathbf{J} = \begin{bmatrix} \mathbf{r}_x^c + \mathbf{A}_x\overline{\mathbf{r}}^p + \mathbf{A}\overline{\mathbf{r}}_x^p & \mathbf{A}\overline{\mathbf{r}}^y & \mathbf{A}\overline{\mathbf{r}}^z \end{bmatrix} \tag{34}$$

where $\overline{\mathbf{r}}^p$ is the local position vector of an arbitrary point on the beam cross-section defined in the local material reference frame:

$$\overline{\mathbf{r}}^p = y\overline{\mathbf{r}}^y + z\overline{\mathbf{r}}^z \tag{35}$$

Using chain rule of differentiation, the gradients along the spatial *x* coordinate in Eq. 34 can be expressed in terms of gradients defined by the differentiation with respect to the arc-length as

$$\mathbf{r}_x = \left(\mathbf{t} + \mathbf{A}_s\overline{\mathbf{r}}^p + \mathbf{A}\overline{\mathbf{r}}_s^p\right)s_x \tag{36}$$

where $s_x = ds/dx$ and **t** is the unit tangent to the beam

centerline given by $\mathbf{t} = d\mathbf{r}^c / ds$. This tangent does not necessarily coincides with the vector **i** in the case of the cross-section frame due to the shear deformation. Using Eqs. 34-36 and utilizing the identities $\mathbf{A}^T\mathbf{A} = \mathbf{I}$ and $\mathbf{t}^T\mathbf{t} = 1$, Green-Lagrange strain components defined in the local material frame can then be written as follows:

$$\varepsilon^{11} = \varepsilon^l + \left(\overline{\mathbf{t}} \cdot \tilde{\overline{\boldsymbol{\kappa}}}\, \overline{\mathbf{r}}^p + \overline{\mathbf{t}} \cdot \overline{\mathbf{r}}_s^p\right)\left(s_x\right)^2 + \varepsilon^{qx}$$

$$\varepsilon^{12} = \frac{s_x}{2}\left(\overline{\mathbf{t}} \cdot \overline{\mathbf{r}}^y + z\overline{\mathbf{r}}^y \cdot \tilde{\overline{\boldsymbol{\kappa}}}\, \overline{\mathbf{r}}^z + \overline{\mathbf{r}}^y \cdot \overline{\mathbf{r}}_s^p\right)$$

$$\varepsilon^{13} = \frac{s_x}{2}\left(\overline{\mathbf{t}} \cdot \overline{\mathbf{r}}^z + y\overline{\mathbf{r}}^z \cdot \tilde{\overline{\boldsymbol{\kappa}}}\, \overline{\mathbf{r}}^y + \overline{\mathbf{r}}^z \cdot \overline{\mathbf{r}}_s^p\right) \qquad (37)$$

$$\varepsilon^{22} = \frac{1}{2}\left(\overline{\mathbf{r}}^y \cdot \overline{\mathbf{r}}^y - 1\right), \quad \varepsilon^{33} = \frac{1}{2}\left(\overline{\mathbf{r}}^z \cdot \overline{\mathbf{r}}^z - 1\right),$$

$$\varepsilon^{23} = \frac{1}{2}\overline{\mathbf{r}}^y \cdot \overline{\mathbf{r}}^z$$

where $\varepsilon^l = \dfrac{ds^2 - dx^2}{2dx^2}$ is the nonlinear longitudinal strain, $\tilde{\overline{\boldsymbol{\kappa}}}$ is the curvature-torsion matrix defined by Eq. 31, $\overline{\mathbf{t}} = \mathbf{A}^T\mathbf{t}$ and ε^{qx} contains the higher order strain components. It is important to note from the strain components defined by Eq. 37 that the deformations of the cross-section due to the change in the gradients along *y* and *z* contribute to all the six strain components defined in the element coordinate system. In some applications in which the effect of deformations of the cross-section is small such as in the case of the cable problems, these deformation modes can introduce undesirable high frequency oscillations that lead to numerical difficulties when the system equations of motion are solved.

Special Case In applications where the effect of deformations of the cross-section is negligible, a special case of the general strain formulation presented in this section can be considered in order to avoid the high frequency oscillations. In the special case discussed in the reminder of this section, the beam cross-section is assumed to remain planar and rigid. In such a case, the strain components defined by Eq. 37 can then be reduced to the following expressions:

$$\varepsilon^{11} = \varepsilon^l + \left(z\overline{\kappa}_2\mathbf{t}\cdot\mathbf{i} - y\overline{\kappa}_3\mathbf{t}\cdot\mathbf{i} + \overline{\kappa}_1\mathbf{t}\cdot\left(y\mathbf{k} - z\mathbf{j}\right)\right)\left(s_x\right)^2$$

$$\varepsilon^{12} = \frac{1}{2}\mathbf{r}_x^c \cdot \mathbf{j} - \frac{s_x}{2}z\overline{\kappa}_1, \quad \varepsilon^{13} = \frac{1}{2}\mathbf{r}_x^c \cdot \mathbf{k} + \frac{s_x}{2}y\overline{\kappa}_1 \qquad (38)$$

$$\varepsilon^{22} = 0, \quad \varepsilon^{33} = 0, \quad \varepsilon^{23} = 0$$

where the fact that $s_x\mathbf{t} = \mathbf{r}_x^c$ is utilized. In such a special case, the local displacement gradient vectors associated with the beam cross-section are always constant and given by

$$\overline{\mathbf{r}}^{y^*} = [0 \quad 1 \quad 0]^T, \qquad \overline{\mathbf{r}}^{z^*} = [0 \quad 0 \quad 1]^T \qquad (39)$$

Using the preceding equation, it is clear that the orthogonality condition $\overline{\mathbf{r}}^y \cdot \overline{\mathbf{r}}^z = 0$ is also satisfied. As a result, the gradients along the *y* and *z* axes can be, respectively, defined by the vectors **j** and **k** of the local material frame as can be shown by Eq. 33. In Eq. 38, the first term of ε^{11} defines the nonlinear strain associated with the elongation along the beam centerline, the second and third terms define the contribution of the in-plane and out-of-plane bending to the axial strain, and the fourth and fifth terms define the contribution of the torsion due to the change in the orientation of the cross-section expressed by $\mathbf{t}\cdot\mathbf{j}$ and $\mathbf{t}\cdot\mathbf{k}$. If the cross-section remains perpendicular to the beam arc-length, these shear effects are identically zero. Furthermore, the shear strain components, ε^{12} and ε^{13}, consist of strains due to the change in the orientation of the cross-section defined by $\frac{1}{2}\mathbf{r}_x^c \cdot \mathbf{j}$ and $\frac{1}{2}\mathbf{r}_x^c \cdot \mathbf{k}$ and the torsional strain $\overline{\kappa}_1$.

6 REISSNER AND EULER-BERNOULLI BEAM MODELS

In this section, it is shown how the Reissner and Euler-Bernoulli finite element beam models can be obtained from the more general theory presented in the preceding section. Since the existing beam models assume planar cross-section, Eq. 38 is used as the starting point for the strain definitions developed in this section. It is important, however, to point out that many of the assumptions used in the models presented in this section can be relaxed when general absolute nodal coordinate models are used. Furthermore, it is shown in this section, how the number of nodal coordinates used in the absolute nodal coordinate formulation can be consistently reduced by developing a set of algebraic constraint equations that can be used to eliminate some of the modes of deformation of the cross-section of the finite element.

Reissner's Beam Model It can be demonstrated that the strain definitions given by Eq. 38 leads to the Reissner's nonlinear beam model [15] that was first used by Simo and Vu-Quoc for geometrically exact finite element beam models [9-11] when the following simplifying assumptions are made:

1. The longitudinal stretch is assumed to be small such that the first order strain can be used as $\varepsilon^l \simeq \mathbf{i}\cdot\left(\mathbf{r}_x^c - \mathbf{i}\right)$.
2. In addition to Assumption 1, the contribution of the longitudinal stretch to the rotation strains is small such that $ds \simeq dx$, that is $s_x = 1$.
3. The contribution of the shear deformation due to the change in the orientation of the cross-section to the bending and torsion is small. As a result, it can be assumed that $\mathbf{t}^T\mathbf{i} \simeq 1$, $\mathbf{t}\cdot\mathbf{j} \simeq 0$ and $\mathbf{t}\cdot\mathbf{k} \simeq 0$ in the definition of the longitudinal strain.

Using the preceding assumptions, the nonlinear strains given by Eq. 38 can be simplified, leading to the following strain expressions used in many geometrically exact finite element beam models [9-11]:

$$\varepsilon^{11} = \mathbf{i}\cdot\left(\mathbf{r}_x^c - \mathbf{i}\right) - y\overline{\kappa}_3 + z\overline{\kappa}_2$$

$$\varepsilon^{12} = \frac{1}{2}\left(\mathbf{r}_x^c \cdot \mathbf{j} - z\overline{\kappa}_1\right), \quad \varepsilon^{13} = \frac{1}{2}\left(\mathbf{r}_x^c \cdot \mathbf{k} + y\overline{\kappa}_1\right) \qquad (40)$$

$$\varepsilon^{22} = 0, \quad \varepsilon^{33} = 0, \quad \varepsilon^{23} = 0$$

Note that using Assumption 2 that approximates *ds* as $ds \simeq dx$ in the terms associated with the rotation strain components, the

local curvature-torsion matrix is approximated by $\tilde{\bar{\boldsymbol{\kappa}}} \simeq \mathbf{A}^T \mathbf{A}_x$. As discussed in the introduction of the paper, the rotation matrix $\mathbf{A}$ in the absolute nodal coordinate formulation is defined by the gradients of the global displacement field given by Eq. 14 or 15, while most of existing geometrically exact finite element beam formulations define the orientation of the cross-section using the independent interpolation of the rotation parameters. This interpolation of the rotation field leads to numerical problems such as the energy drift and violation of the principle of work and energy.

The preceding assumptions used to obtain Reissner's beam model imply that the beam cross-section remains planar, but the cross-section does not necessarily remain perpendicular to the beam centerline. As a result, the condition given by Eq. 39 is imposed in order to eliminate the strain components associated with the deformation of the cross-section. In such a case, the following conditions can be used:

$$\mathbf{C} = \begin{bmatrix} \mathbf{r}_y \cdot \mathbf{r}_y - 1 \\ \mathbf{r}_z \cdot \mathbf{r}_z - 1 \\ \mathbf{r}_y \cdot \mathbf{r}_z \end{bmatrix} = \mathbf{0} \tag{41}$$

where the preceding three scalar equations guarantee that $\varepsilon^{22} = \varepsilon^{33} = \varepsilon^{23} = 0$ and eliminate the modes of deformation of the cross-section, as discussed in Sections 5. Recall that the general motion of an infinitesimal volume can be described using twelve independent parameters: three translational parameters; three rotational parameters to describe the reference orientation of the volume; and six parameters that define six strain components. As a consequence, three of the six strain components associated with the deformation of the cross-section can be eliminated using Eq. 41.

Euler-Bernoulli Beam Model When the assumptions of Euler-Bernoulli Beam theory are used, the vector $\mathbf{i}$ is always tangent to the space curve that defines the centerline of the beam. For this reason, the vector tangent to the beam centerline, $\mathbf{r}_x^c$, is perpendicular to the vectors $\mathbf{j}$ and $\mathbf{k}$, leading to the following definitions deduced from the strain components given by Eq. 40:

$$\begin{aligned} \varepsilon^{11} &= \mathbf{i} \cdot \left(\mathbf{r}_x^c - \mathbf{i} \right) - y\bar{\kappa}_3 + z\bar{\kappa}_2 \\ \varepsilon^{12} &= -\frac{1}{2} z\bar{\kappa}_1, \quad \varepsilon^{13} = \frac{1}{2} y\bar{\kappa}_1 \\ \varepsilon^{22} &= 0, \quad \varepsilon^{33} = 0, \quad \varepsilon^{23} = 0 \end{aligned} \tag{42}$$

In such a case, the shear strain components $\frac{1}{2}\mathbf{r}_x^c \cdot \mathbf{j}$ and $\frac{1}{2}\mathbf{r}_x^c \cdot \mathbf{k}$ are equal to zero in order for $\mathbf{r}_x^c$ to remain normal to the cross section of the beam, leading to the Euler-Bernoulli strain measure. As a result, an Euler-Bernoulli beam element can be obtained in the absolute nodal coordinate formulation using the following two additional conditions imposed on the displacement of a material point within an element:

$$\mathbf{C} = \begin{bmatrix} \mathbf{r}_y \cdot \hat{\mathbf{r}}_x^c \\ \mathbf{r}_z \cdot \hat{\mathbf{r}}_x^c \end{bmatrix} = \mathbf{0} \tag{43}$$

Note that the gradient vectors $\mathbf{r}_y$ and $\mathbf{r}_z$ are, respectively, equal to $\mathbf{j}^o$ and $\mathbf{k}^o$ under the conditions given by Eq. 41 and Eq. 43 guarantees that shear strain components at the material point given by Eq. 40 are equals to zero; that is

$$\frac{1}{2}\mathbf{r}_x^c \cdot \mathbf{j}^o = 0, \qquad \frac{1}{2}\mathbf{r}_x^c \cdot \mathbf{k}^o = 0 \tag{44}$$

As a result, the virtual work of the elastic forces can be simply written as

$$\delta W = \int_0^\ell (EA\varepsilon^l \delta\varepsilon^l + GI_{xx}\,\bar{\kappa}_1 \delta\bar{\kappa}_1 + EI_{yy}\,\bar{\kappa}_2 \delta\bar{\kappa}_2 + EI_{zz}\,\bar{\kappa}_3 \delta\bar{\kappa}_3) dx \tag{45}$$

where E is Young's modulus, A is cross-section area, G is the modulus of rigidity, I_{xx} is polar moment of area, and I_{yy} and I_{zz} are second moments of area. The strain components are defined in this case by

$$\varepsilon^l = \frac{1}{2}\left(\mathbf{r}_x^c \cdot \mathbf{r}_x^c - 1 \right), \quad \bar{\kappa}_1 = \mathbf{k}^o \cdot \mathbf{j}_x, \quad \bar{\kappa}_2 \simeq -\mathbf{k}^o \cdot \mathbf{r}_{xx}^c, \quad \bar{\kappa}_3 \simeq \mathbf{j}^o \cdot \mathbf{r}_{xx}^c \tag{46}$$

where the one-dimensional Green strain instead of the first order approximation used in Eq. 42 is employed for the longitudinal stretch. Furthermore, if the constraint condition of Eq. 41 is satisfied, $\mathbf{j}^o = \mathbf{r}_y$ and $\mathbf{k}^o = \mathbf{r}_z$, leading to the simpler definition of the elastic forces.

7 NUMERICAL EXAMPLE

In this section, numerical examples are presented in order to demonstrate the use of different strain definitions that also lead to the use of different numbers of independent nodal coordinates of the finite element. In order to demonstrate the effect of the cross-section deformation modes, the constraint formulation is used to impose the Euler-Bernoulli beam assumptions as discussed in Sections 6. Furthermore, a lower order beam element based on the absolute nodal coordinate formulation which is a special case of the formulation presented in [7] is used for the purpose of comparison. In the case of the higher order element, for simplicity, the constraint equations used for Euler-Bernoulli beam assumptions are imposed at the nodal points only. That is, Eqs. 41 and 43 hold only at the nodal points. A similar, but conceptually different procedure is used in the literature [16] for an orthonormality condition of direction cosine coordinates. In the following examples, three different finite element models are used: the first model (Model I) uses the higher order 24 nodal coordinate element as originally presented in the literature [1]; the second model (Model II) imposes the Euler-Bernoulli beam assumptions to Model I in order to consistently eliminate deformation modes of the cross-section as discussed in this investigation; and the third model (Model III) is a reduced order beam element obtained using six nodal coordinates at each node; three translations and the gradient vector along the x coordinate as presented in the literature [7].

A cantilever beam presented in the literature [17,18] is considered in this example. The length, height and width of the beam are assumed to be 2.4 m, 9 mm and 0.2 m, respectively. Young's modulus is assumed to be 1.0E+6 N/m^2, while the material density is 2770 kg/m^3. A concentrated vertical force is applied at the free end as follows [17]:

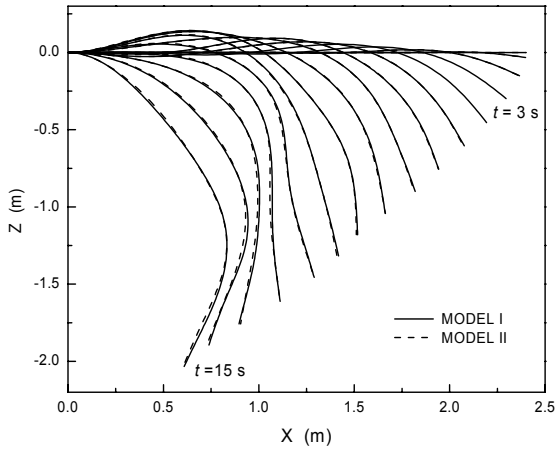

Fig. 2 Deformed shapes of the large deformation cantilever beam problem

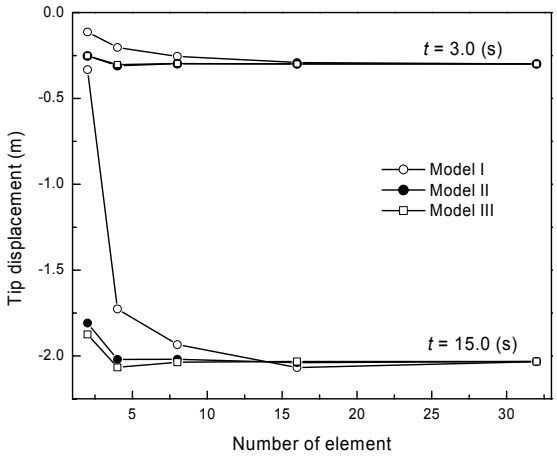

Fig. 3 Effect of the number of elements

$$F(t) = \begin{cases} \dfrac{F_0}{2}\left(1-\cos t\right) & t<1 \\ F_0 & t\geq 1 \end{cases} \tag{47}$$

where F_0 = 0.09 N. Figure 2 shows the deformed shapes of the cantilever beam obtained using 32 elements of Model I and II. In Figure 3, the vertical tip displacements at time 3 s and 15 s are presented for different number of finite elements. The results presented in this figure shows that all the Models lead to the convergent solution as the number of elements increases. However, for this thin beam problem, the rate of convergence in the case of Model II and III is better than that of Model I. As discussed in Section 4 for the particular beam element used in this study, the bending strains can be defined in Model I using the derivatives of $\mathbf{r}_y$ and $\mathbf{r}_z$ that are approximated by linear polynomials when Green-Lagrange strains (see Eq. 8) or the first order strains (see Eq. 23) are used. On the other hand, the curvature expression given by Eq. 46 used in Model II and III are defined using the derivatives of $\mathbf{r}^c$ approximated by cubic polynomials. As a result, Models II and III lead to better convergence for the bending strains and their solutions are in good agreement since both models employ the same strain expressions and simplifying assumptions, despite the fact that the two models use different numbers of nodal coordinates and different numerical solution procedures. In terms of efficiencies, since Models II leads to better convergence for the bending strains than those of Model I in the thin beam problem, CPU time of Model II is approximately 11 times faster than that of Model I in this specific problem. Furthermore, if one further reduces the thickness of the beam and increases the stiffness, the difference in CPU time becomes more significant.

In the second example, the height of the cross-section is increased to 0.4 m in order to discuss the effect of the deformation of the cross-section. The external force is also increased to F_0=180 N. Figure 4 shows the norm of the gradient along z at the middle point used to define the stretch of the cross-section. As can be seen from these figures, the

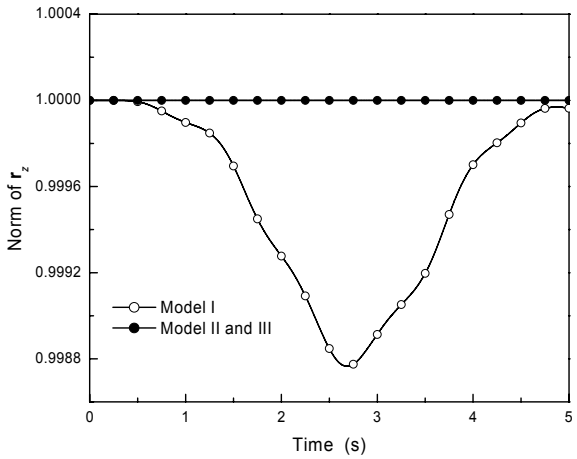

Fig. 4 Norm of the gradient along z

deformation of the cross-section in this problem may not be neglected and Model I must be used for such a problem. Note also that, in the case of plasticity problems, since the material deformation is defined in a deviatoric stress/strain space, deformation of the cross-section described by $\mathbf{r}_y$ and $\mathbf{r}_z$ are used in the absolute nodal coordinate formulation and these position vector gradients are not neglected in such a problem [19].

8 SUMMARY AND CONCLUSIONS

The deformation modes for a three-dimensional beam element obtained using the finite element absolute nodal coordinate formulation is discussed in this paper. Using the deformation modes discussed in this investigation, a procedure for eliminating modes of deformation of the finite element is presented. The coordinate reduction procedure presented in this paper requires introducing local frames such as the tangent frame and the cross section frames. The strain components can be defined in these local frames, leading to strain definitions

that can be used to obtain, by imposing appropriate assumptions, the simpler models such as the Reissner and Euler-Bernoulli beam models. The assumptions used to define these models lead to the definition of the algebraic constraint equations that can be used to define a set of dependent coordinates eliminated, thereby reducing the degrees of freedom of the finite element. This coordinate reduction procedure ensures the continuity of the gradients at the nodal points and also leads to the definition of a unique displacement field. Numerical examples are presented in order to demonstrate the use of the beam model obtained using Euler-Bernoulli beam assumptions and these results are compared with those obtained using more general models in the absolute nodal coordinate formulation. Lower order finite elements based on the absolute nodal coordinate formulation have been also proposed in the literature [5-7]. These elements, as used in the analysis of thin beam and plate structures without the need for imposing algebraic constraint equations to eliminate high frequency cross-section modes of deformation.

REFERENCES

1 Shabana, A. A. and Yakoub, R. Y., 2001, "Three Dimensional Absolute Nodal Coordinate Formulation for Beam Elements", *ASME Journal of Mechanical Design*, vol. 123, pp. 606-621.

2 Bonet, J. and Wood, R.D., 1997, *Nonlinear Continuum Mechanics for Finite Element Analysis*, University Press, Cambridge.

3 Sugiyama, H., and Shabana, A. A., 2004, "On the Use of Implicit Integration Methods and the Absolute Nodal Coordinate Formulation in the Analysis of Elasto-Plastic Deformation Problems", *Nonlinear Dynamics*, vol. 37, pp. 245-270.

4 Garcia-Vallejo, D., Mayo, J., Escalona, J. L. and Dominguez, J., 2004, "Efficient Evaluation of the Elastic Forces and the Jacobian in the Absolute Nodal Coordinate Formulation", *Nonlinear Dynamics*, vol. 35, pp. 313-329.

5 Christensen, A.P. and Shabana, A. A., 1998, "Exact Modeling of the Spatial Rigid Body Inertia Using the Finite Element Method", *ASME Journal of Vibration and Acoustics*, vol. 120, pp. 650-657.

6 Von Dombrowski, S., 2002, "Analysis of Large Flexible Body Deformation in Multibody Systems Using Absolute Coordinates", *Multibody System Dynamics*, vol. 8, pp. 409-432.

7 Dmitrochenko, O. N. and Pogorelov, D. Y., 2003, "Generalization of Plate Finite Elements for Absolute Nodal Coordinate Formulation", *Multibody System Dynamics*, vol. 10, pp. 17-43.

8 Sugiyama, H., Gerstmayr, J. and Shabana, A. A., 2005, "Deformation Modes of the Finite Element Cross-Section", *Technical Report # MBS05-2-UIC,* Department of Mechanical Engineering, University of Illinois at Chicago.

9 Simo, J. C. and Vu-Quoc, L., 1986, "Three-Dimensional Finite-Strain Rod Model. Part II: Computational Aspects." *Computer Methods in Applied Mechanics and Engineering*, vol. 58, pp. 79-116.

10 Cardona, A. and Geradin, M., 1988, "A Beam Finite-Element Non-Linear Theory with Finite Rotations", *International Journal for Numerical Methods in Engineering*, vol. 26, pp. 2403-2438.

11 Ibrahimbegovic, A., 1995, "On Finite Element Implementation of Geometrically Nonlinear Reissner's Beam Theory: Three-Dimensional Curved Beam Elements", *Computer Methods in Applied Mechanics and Engineering*, vol. 122, pp. 11-26.

12 Sugiyama, H., Escalona, J. L. and Shabana, A. A., 2003, "Formulation of Three-Dimensional Joint Constraints Using the Absolute Nodal Coordinates", *Nonlinear Dynamics*, vol. 31, pp. 167-195.

13 Sopanen, J. T. and Mikkola, A. M., 2003, "Description of Elastic Forces in Absolute Nodal Coordinate Formulation", *Nonlinear Dynamics*, vol. 34, pp. 53-74.

14 Greenberg, M. D., 1998, *Advanced Engineering Mathematics*, 2nd, Prentice Hall, Upper Saddle River, N.J.

15 Reissner, E., 1981, "On finite Deformations of Space-Curved Beams", *Journal of Applied Mathematics and Physics (ZAMP)*, vol. 32, pp. 734-744.

16 García de Jalón, J. and Bayo, E., 1994, *Kinematic and Dynamic Simulation of Multibody Systems*, Springer-Verlag, New York.

17 Iwai, R. and Kobayashi, N., 2003, "A New Flexible Multibody Beam Element Based on the Absolute Nodal Coordinate Formulation Using the Global Shape Function and the Analytical Mode Shape Function", *Nonlinear Dynamics*, vol. 34, pp. 207-232.

18 Shabana, A. A., Hussien, H. A. and Escalona, J. L., 1998, "Application of the Absolute Nodal Coordinate Formulation to Large Rotation and Large Deformation Problems", *ASME Journal of Mechanical Design*, vol. 120, pp. 188-195.

19 Sugiyama, H., and Shabana, A. A., 2004, "Application of Plasticity Theory and Absolute Nodal Coordinate Formulation to Flexible Multibody System Dynamics", *ASME Journal of Mechanical Design*, vol. 126, pp. 478-487.